P-doping and efficient carrier injection induced by graphene oxide for high performing WSe_2 rectification devices

Muhammad Atif Khan,[1] Servin Rathi,[1] Inyeal Lee,[1] Lijun Li,[1] Dongsuk Lim,[2] Moonshik Kang,[1,3] and Gil-Ho Kim[1,a)]

[1]*School of Electronic and Electrical Engineering and Sungkyunkwan Advanced Institute of Nanotechnology (SAINT), Sungkyunkwan University, Suwon 16419, South Korea*
[2]*School of Advanced Materials Science and Engineering, Sungkyunkwan University, Suwon 16419, South Korea*
[3]*Manufacturing Engineering Team, Memory Division, Samsung Electronics Co., Hwasung 18396, South Korea*

(Received 24 November 2015; accepted 16 February 2016; published online 1 March 2016)

In this work, we fabricated multi-layer WSe_2 rectifying diodes using graphene oxide (GO) as p-doping material on one side of the contacting electrodes. This GO layer can reduce the contact resistance by forming a tunneling barrier for efficient hole injection, while it increases the contact resistance for the injection of electrons. Results of Raman shift spectra and the opto-electric response of the device confirmed the p-doping effect caused by the GO layer and the formation of a barrier, respectively. We observed a gate tunable rectification effect with a forward/reverse current ratio of 10^4 and low reverse bias current of 10^{-10} A. Applying a GO layer in the fabrication of two-dimensional transition metal dichalcogenides based devices is a very useful method in the applications in future nanotechnologies. © *2016 AIP Publishing LLC*.
[http://dx.doi.org/10.1063/1.4942888]

Transition metal dichalcogenides (TMDCs) are strong candidates for future electronics applications because of their obtainable atomic layer thickness, large band gaps (1–2 eV), and gate tunable electrical properties.[1] In two-dimensional (2D) TMDCs, the absence of surface dangling bonds, the dielectric-mediated mobility, and the reduced short channel effects render them a class of electrically favorable materials for transistor applications. In addition to these qualities, the quantum confinement of carriers within an atomic channel thickness (monolayer) holds potential applications in quantum devices. These advantages make them a strong candidate to replace the conventional Si devices in semiconductor technology.[2,3] WSe_2 (tungsten diselenide) is one of the prominent members of the TMDC family, with a bulk indirect band gap of ~1.2 eV.[4,5] As WSe_2 demonstrates ambipolar behaviour[6,7] which limits its digital and analog applications, the doping techniques are critical for a successful realization of TMDC materials in practical devices.

Due to the atomic nature of TMDCs, the current fabrication techniques like ion implantation and diffusive doping are difficult to implement for the realization of basic junction devices. However, surface doping and doping by strain control in WSe_2 have been reported for FETs[8–11] and diode applications using van der Waals assembly, e.g., p-n junctions realized in WSe_2/MoS_2 heterostrucures[12,13] and InAs/WSe_2 heterostructure,[14] and theoretically suggested for graphene and TMDCs.[15] Moreover, h-BN has also been used along with graphene and TMDC for its application in tunneling, encapsulation, and split gate induced p-n junction.[16–19] These works used heterostructures formed by the complex procedure of wet or dry transfer of TMDC atomic layers which involves van der Waals interaction in layered materials. Rectifying effect had also been achieved by fluoropolymer encapsulation of the TMDC layers or by applying a liquid gate.[20,21]

In this study, we report a very simple method to achieve rectification behavior in WSe_2 by applying graphene oxide (GO) on one side of the contact area as shown in Fig. 1(a) (see supplementary material for methods and AFM data of device[22]). GO is a sheet of carbon atoms (graphene) with randomly attached oxygen functional groups mostly in the form of epoxies and hydroxyls. The presence of these oxygen functional groups makes it an insulator because oxygen disrupts the sp^2 hybridization in graphene. Production of GO is very simple and inexpensive by widely used Hummers' method. It would be a great economical advantage if GO can be used along with TMDC in future industrial production of nano electronic devices.[23]

Rectification behavior was observed with the device, showing an I_{on}/I_{off} ratio of 10^4 and an I_{off} in the range of 10^{-10} A. These values are comparable to previous reports on rectification devices achieved in TMDC.[24] Upon light exposure, the device exhibits strong photo-electric effect, with an open circuit voltage and a short circuit current, which are typical features of a p-n junction diode.

Fig. 1(c) presents a comparison between the drain current-drain voltage (I-V) curves of a typical two probe WSe_2 device of pristine layer and the device fabricated with GO doping on one side of the contact. It is obvious that in the normal two probe device, the I-V curve is symmetric (see supplementary material for I-V plot at different gate voltages[22]). The device fabricated with GO shows asymmetric I-V characteristic. It flows negligibly small current ~0.02 nA, at positive V, and relatively larger current (~100 nA), at negative V.

a)Electronic mail: ghkim@skku.edu

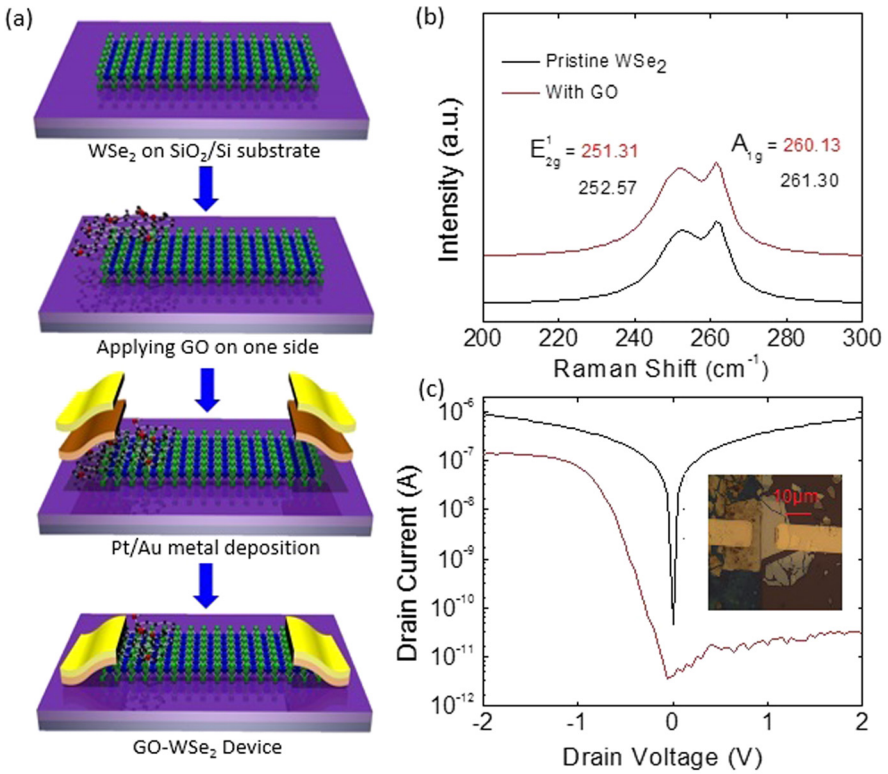

FIG. 1. (a) Schematic drawing showing the steps involved in fabrication of one side GO covered WSe_2 device. (b) Raman spectra of pristine WSe_2 and WSe_2 covered with GO. (c) Plot of drain current-drain voltage of pristine WSe_2 and GO-WSe_2 device in semi-logarithmic scale. The inset shows an optical image of the GO treated WSe_2 device.

Figs. 2(a) and 2(b) present the *I-V* curves of the device with half side GO doping at different gate voltages. All measurements were performed by connecting the ground terminal to the electrode on GO side and applying bias to the electrode on the other side. The device shows a clear p-type characteristic (hole dominated transport) with $I_{on}/I_{off} \sim 10^4$ in an applied voltage range of -2 V to 2 V. Here, I_{on} and I_{off} are current values at $V = -2$ V and $V = 2$ V, respectively. The *I-V* characteristics of the device show a strong dependence on gate voltage (V_g). At $V_g = 50$ V, the device remains in off state with a maximum current of $\sim 10^{-10}$ A. The maximum to minimum current ratio is around one order of magnitude. At positive gate voltages, carriers (holes) are depleted and the device is in off state for all values of drain voltage. At $V_g = 0$ V, the device shows a decent I_{on}/I_{off} value of 10^4 with $I_{on} \sim 10^{-7}$ A, and $I_{off} \sim 10^{-11}$ A. At $V_g = -50$ V, I_{on} and I_{off} are both increased by one order of magnitude, while the ratio of I_{on}/I_{off} remains roughly the same ($\sim 10^4$). We observed high current with

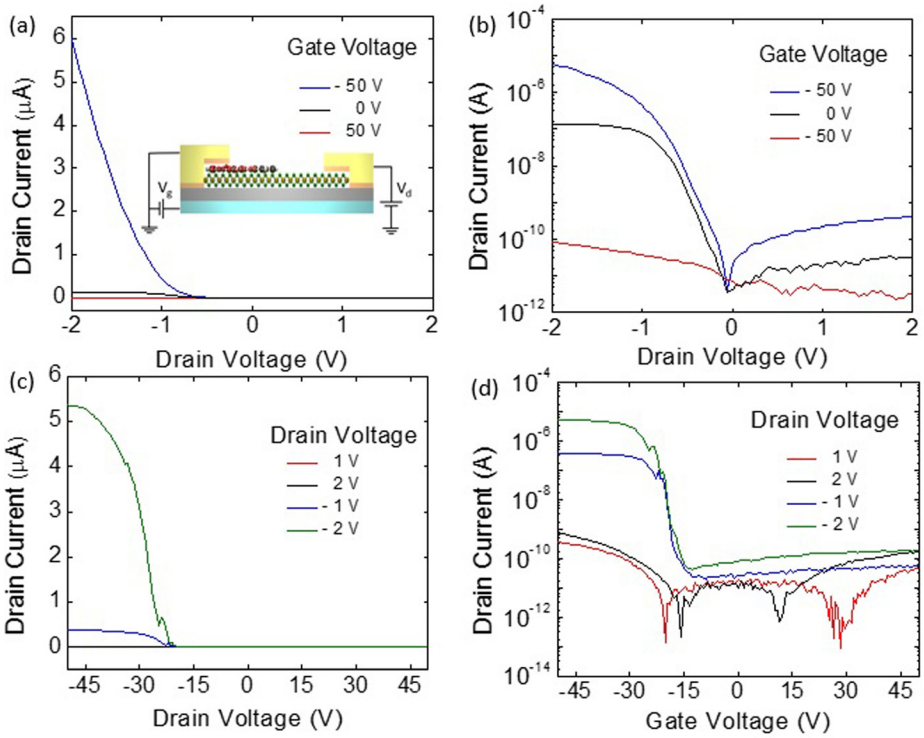

FIG. 2. (a) Plot of absolute value of drain current as a function of drain voltage at different gate voltages. (b) Re plot of curves in (a) in semi-logarithmic scale. (c) Plot of absolute value of drain current as a function of back gate voltage at different drain voltages. (d) Re-plot of curves in (c) in semi-logarithmic scale.

negative V_g and low current with positive V_g, which indicates that current conduction is via holes.

Figs. 2(c) and 2(d) are plots showing the change in drain current when the back gate voltage is swept at various drain voltages. We observed that the device has a very small I_{on}/I_{off} ratio while sweeping the gate voltage at positive drain voltages (V). Here, I_{on} means drain current at $V_g = -50$ V and I_{off} means drain current at $V_g = 50$ V. The maximum current observed with positive V is of the order of nano-amperes even at V_g as high as -50 V. Thus, we can deduce that the device is in off state for positive drain biases. On the other hand, prominent carrier transport and I_{on}/I_{off} ratio for negative drain biases is observed, with I_{on} of order of 10^{-5} A and I_{on}/I_{off} ratio of 10^4. This again proves that the transport is unidirectional and takes place for negative drain bias only.

Next, we discuss the physical mechanism responsible for the rectifying characteristics of the device. The rectifying behavior can be due to two reasons: (1) the doping of WSe_2 caused by GO forms a barrier between pristine and doped WSe_2. (2) GO is on one contact only, the rectification could be due to the asymmetry in contacts on both sides.

It had been explained earlier that GO can p-dope TMDC.[25] GO contains high electronegative species like O and OH. These species can take electrons from WSe_2 which is equivalent to giving holes or p doping. In Raman spectra, p doping results in a blue-shift of the two characteristic peaks E^1_{2g} and A_{1g}.[26–28] In our experiment, the Raman data show that when WSe_2 was covered with GO, these two peak positions blue shifted of 1.25 cm^{-1} compared to the results of the pristine layer (see Fig. 1(b)).

It can be confirmed that the WSe_2 covered by GO is p-doped while the uncovered WSe_2 is ambipolar. On the doped side, there is higher density of holes than that in intrinsic WSe_2. The difference in carrier concentration on both sides causes the electrons to diffuse from intrinsic side to doped side and a barrier is formed as a result of band bending (see illustration in Fig. 3(b)). When a positive voltage is applied to the drain terminal, the barrier height is increased and a very small current flows through—the device switches to off state (Fig. 3(c)). When the drain terminal is biased negatively, the barrier height is reduced and the current starts to flow through - the device switches to on state (Fig. 3(d)).

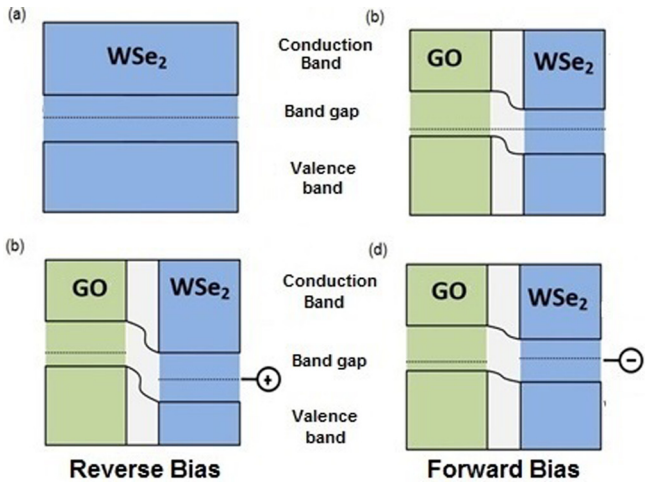

FIG. 3. (a) Schematic drawing showing band structure of pristine WSe_2. (b) Schematic illustrating the formation of barrier between pristine and GO treated WSe_2. (c) Alignment of band structure in reverse bias. (d) Alignment of band structure in forward bias.

To verify the existence of a barrier, the device was illuminated with laser to study the characteristics of the flow of the photo-induced charge carriers. The opto-electronic response of the device plotted in Fig. 4 exhibits the feature of a typical p-n junction diode. Under illumination of laser light, two prominent changes in drain current were observed: first, the reverse current is increased. Second, the I-V curves shifted to the left; therefore, an open circuit voltage and a short circuit current can be determined. These effects are due to photo excited electron-hole pairs. Due to drain bias, these electron and hole carriers move towards the opposite contacts.

The maximum value of the open circuit voltage is 0.35 V, and the maximum value of short circuit current is 9 nA. We have calculated responsivity and specific detectivity of the device. Responsivity is the ratio of photo current to incident optical power, $R = I_{ph}/P_{in}$, and specific detectivity (D^*) is calculated by $D^* = A^{1/2}/NEP$, where A is the illuminated area and NEP is the noise equivalent power, $NEP = (2qI)^{1/2}/R$.[29] Specific detectivity enables the comparison of device with different geometry. The maximum obtained value of responsivity is 80 A/W at $V = -2$ V, and in the absence of applying a gate bias, while the maximum value of detectivity is 3×10^{11} Jones. These values are comparable to previous published data on TMDC based photo detectors.[24,29] Moreover, it can be seen in Fig. 4(d) that when the device is forward biased, the ratio of $(I_{laser} - I_{dark})$ to I_{dark} has smaller values because of a larger I_{dark}, but in reverse bias, this ratio is much higher because I_{dark} is smaller and I_{laser} becomes prominent; here, I_{laser} is drain current when the device is illuminated by laser.

To further investigate the doping behavior of GO on WSe_2, we fabricated multilayer WSe_2 FET and applied GO only in the channel region of the device. The comparison of the device characteristics before and after the application of GO is presented in Fig. 5(a) (see supplementary material for I-V characteristics[22]). The effect of GO doping is not very strong and only renders a slight increase in current. Thus high rectification is not expected with only the junction effect of GO doped WSe_2 and pristine WSe_2. Next, we look at the rectification behavior due to asymmetry of contacts with GO on one side and only metal on the other side.

Fig. 5(b) is a plot of $ln\ (I/V^2)$ as a function of $1/V$. It gives an insight in carrier transport at contacts where I and V are drain current and drain voltage, respectively.[30] The linear region of the plot indicates Fowler–Nordheim (F-N) tunneling, and the exponential region indicates direct tunneling.[30] It is obvious that GO plays the role of a tunneling barrier and can enable efficient injection of holes. It has been reported that a dielectric can be used as the tunneling barrier between the metal and the semi-conductor for efficient injection of carriers. It can also reduce the barrier height at metal semiconductor interface by alleviating the Fermi level pinning.[31–33] Due to efficient injection of carriers, the contact with GO has better performance. When the holes are injected from this contact, a larger current was observed. When the bias voltage is reversed, the carriers experience higher contact resistance; hence, a smaller current and poor performance of device were seen.

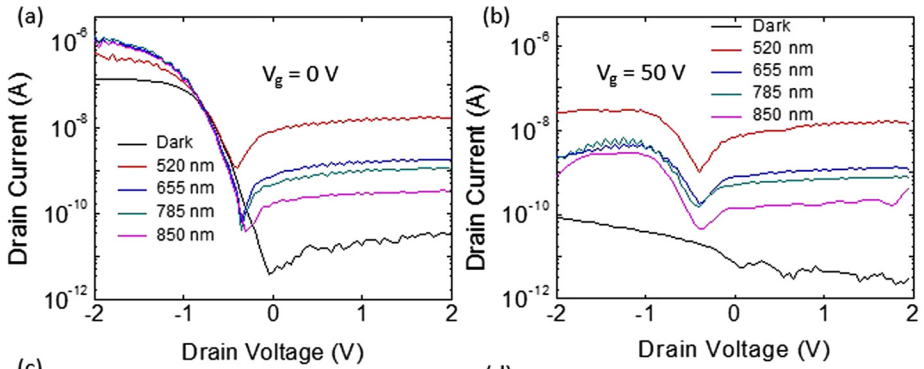

FIG. 4. Plot of drain current as a function of drain voltage under illumination in semi-logarithmic scale at (a) 0 V gate bias, (b) 50 V gate bias, (c) −50 V gate bias. (d) Plot of $(I_{laser} - I_{dark})/I_{dark}$ at 0 V gate bias in semi logarithmic scale.

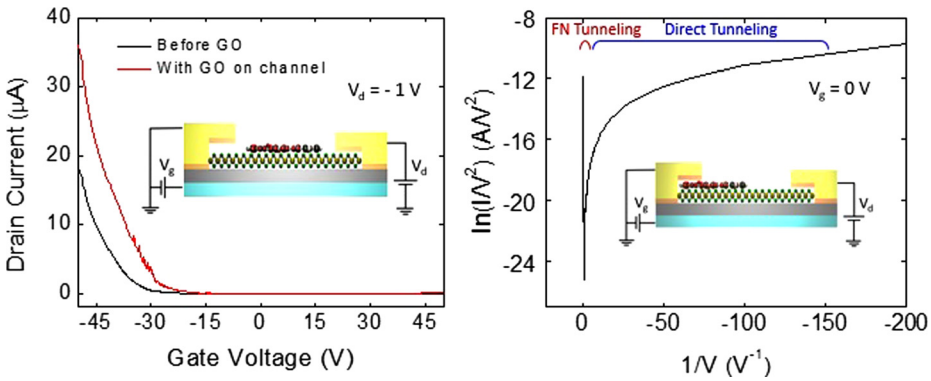

FIG. 5. (a) Drain current-drain voltage characteristics of device before and after covering the channel region with GO as illustrated in the inset image. (b) Plot of $ln\ (I/V^2)$ versus $1/V$ of the device as shown in inset image.

Therefore, the rectification observed in the device can be attributed to the combined effect of barrier formation, at pristine and GO treated WSe_2 junction, and asymmetrical contacts due to deposition of GO on one of the contacts. At forward bias, the holes are injected efficiently at the GO-tunneling contact and are transported across the lowered p-n junction barrier resulting in high drain current. However, under reverse bias, a lower carrier injection at the metal contact combined with higher barrier at the junction results in lowering of the device current. Thus the device can be assessed as a junction diode in series with an asymmetric contact resistor, where both are contributing to the rectification property of the device, although the relative contribution of these parameters to the observed rectification cannot be taken into account in the present two terminal device layout.

In conclusion, a facile technique was introduced to fabricate rectifying diode from multilayer WSe_2. GO can not only p-dope WSe_2 but can also improve the contact resistance of the device by providing a suitable barrier for efficient hole injection. The device exhibits highly rectifying properties and strong optoelectronic response. An on/off ratio as high as 10^4 was observed when doping with GO on one side of the contact. This study demonstrates that the technique combining GO and TMDCs has very promising applications in fabricating high performance and low cost 2D nano-devices, which may reveal a wholly different avenue in semiconductor manufacturing industry.

This research was supported by the Basic Science Research Program through the National Research Foundation of Korea (NRF) funded by the Ministry of Education, Science, and Technology (2013R1A2A2A01069023).

[1]Q. H. Wang, K. K. Zadeh, A. Kis, J. N. Coleman, and M. S. Strano, Nat. Nanotechnol. **7**, 699–712 (2012).
[2]D. Jariwala, V. K. Sangwan, L. J. Lauhon, T. J. Marks, and M. C. Hersam, ACS Nano **8**, 1102–1120 (2014).
[3]B. Radisavljevic, A. Radenovic, J. Brivio, V. Giacometti, and A. Kis, Nat. Nanotechnol. **6**, 147–150 (2011).
[4]H. Jiang, J. Phys. Chem. C **116**, 7664–7671 (2012).
[5]G. H. Yousefi, Mater. Lett. **9**, 38–40 (1989).
[6]J. K. Huang, J. Pu., C. L. Hsu, M. H. Chiu, Z. Y. Juang, Y. H. Chang, W. H. Chang, Y. Iwasa, T. Takenobu, and L. J. Li, ACS Nano **8**, 923–930 (2014).
[7]V. Podzorov, M. E. Gershenson, C. Kloc, R. Zeis, and E. Bucher, Appl. Phys. Lett. **84**, 3301 (2004).
[8]K. Chen, D. Kiriya, M. Hettick, M. Tosun, T. J. Ha, S. R. Madhvapathy, S. Desai, A. Sachid, and A. Javey, APL Mater. **2**, 92504 (2014).

[9]H. J. Chuang, X. Tan, N. J. Ghimire, M. M. Perera, B. Chamlagain, M. M. C. Cheng, J. Yan, D. Mandrus, D. Tomanek, and Z. Zhou, Nano Lett. **14**, 3594–3601 (2014).
[10]H. Fang, S. Chuang, T. C. Chang, K. Takei, T. Takahashi, and A. Javey, Nano Lett. **12**, 3788−3792 (2012).
[11]B. Amin, T. P. Kaloni, and U. Schwingenschlogl, RSC Adv. **4**, 34561–34565 (2014).
[12]C. H. Lee, G. H. Lee, A. M. V. Zande, W. Chen, Y. Li1, M. Han, X. Cui, G. Arefe, C. Nuckolls, T. F. Heinz, J. Guo, J. Hone, and P. Kim, Nat. Nanotechnol. **9**, 676–681 (2014).
[13]R. Cheng, D. Li, H. Zhou, C. Wang, A. Yin, S. Jiang, Y. Liu, Y. Chen, Y. Huang, and X. Duan, Nano Lett. **14**, 5590−5597 (2014).
[14]S. Chuang, R. Kapadia, H. Fang, T. C. Chang, W. C. Yen, Y. L. Chueh, and A. Javey, Appl. Phys. Lett. **102**, 242101 (2013).
[15]T. P. Kaloni, L. Kou, T. Frauenheim, and U. Schwingenschlogl, Appl. Phys. Lett. **105**, 233112 (2014).
[16]A. Mishchenko, J. S. Tu, Y. Cao, R. V. Gorbachev, J. R. Wallbank, M. T. Greenaway, V. E. Morozov, S. V. Morozov, M. J. Zhu, S. L. Wong, F. Withers, C. R. Woods, Y-J. Kim, K. Watanabe, T. Taniguchi, E. E. Vdovin, O. Makarovsky, T. M. Fromhold, V. I. Fal'ko, A. K. Geim, L. Eaves, and K. S. Novoselov, Nat. Nanotechnol. **9**, 808–813 (2014).
[17]T. P. Kaloni, Y. C. Cheng, and U. Schwingenschlogl, J. Mater. Chem. **22**, 919–922 (2012).
[18]T. P. Kaloni, R. P. Joshi, N. P. Adhikari, and U. Schwingenschlogl, Appl. Phys. Lett. **104**, 73116 (2014).
[19]J. S. Ross, P. Klement, A. M. Jones, N. J. Ghimire, J. Yan, D. G. Mandrus, T. Taniguchi, K. Watanabe, K. Kitamura, W. Yao, D. H. Cobden, and X. Xu, Nat. Nanotechnol. **9**, 268–272 (2014).
[20]Y. J. Zhang, J. T. Ye, Y. Yomogida, T. Takenobu, and Y. Iwasa, Nano Lett. **13**, 3023−3028 (2013).
[21]P. J. Jeon, S. W. Min, J. S. Kim, S. R. A. Raza, K. Choi, H. S. Lee, Y. T. Lee, D. K. Hwang, H. J. Choi, and S. Im, J. Mater. Chem. C **3**, 2751 (2015).
[22]See supplementary material at http://dx.doi.org/10.1063/1.4942888 for AFM data and I-V characteristics of devices.
[23]K. P. Loh, Q. Bao, G. Eda, and M. Chhowalla, Nat. Chem. **2**, 1015–1024 (2010).
[24]M. S. Choi, D. Qu, D. Lee, X. Liu, K. Watanabe, T. Taniguchi, and W. J. Yoo, ACS Nano **8**, 9332–9340 (2014).
[25]T. Musso, P. V. Kumar, A. S. Foster, and J. C. Grossman, ACS Nano **8**, 11432–11439 (2014).
[26]C. H. Chen, C. L. Wu, J. Pu, M. H. Chiu, P. Kumar, T. Takenobu, and L. J. Li, 2D Mater. **1**, 034001 (2014).
[27]K. P. Dhakal, D. L. Duong, J. Lee, H. Nam, M. Kim, M. Kan, Y. H. Lee, and J. Kim, Nanoscale **6**, 13028 (2014).
[28]Y. Shi, J. K. Huang, L. Jin, Y. T. Hsu, S. F. Yu, L. J. Li, and H. Y. Yang, Sci. Rep. **3**, 1839 (2013).
[29]S. Rathi, I. Lee, D. Lim, J. Wang, Y. Ochiai, N. Aoki, K. Watanabe, T. Taniguchi, G. H. Lee, Y. J. Yu, P. Kim, and G. H. Kim, Nano Lett. **15**, 5017−5024 (2015).
[30]F. Ahmed, M. S. Choi, X. Liu, and W. J. Yoo, Nanoscale **7**, 9222 (2015).
[31]A. Dankert, L. Langouche, M. V. Kamalakar, and S. P. Dash, ACS Nano **8**, 476–482 (2014).
[32]J. Y. J. Lin, A. M. Roy, A. Nainani, Y. Sun, and K. C. Saraswat, Appl. Phys. Lett. **98**, 92113 (2011).
[33]Y. Zhou, W. Han, Y. Wang, F. Xiu, J. Zou, R. K. Kawakami, and K. L. Wang, Appl. Phys. Lett. **96**, 102103 (2010).